INTERNATIONAL JOURNAL OF AUTOMOTIVE AND MECHANICAL ENGINEERING (IJAME)
ISSN: 2229-8649 e-ISSN: 2180-1606
VOL. 19, ISSUE 2, 9734 – 9746
DOI: https://doi.org/10.15282/ijame.19.2.2022.09.0751

ORIGINAL ARTICLE

Solid-State Diffusion Welding of Commercial Aluminum Alloy with Pure Copper

W. Bedjaoui[1], Z. Boumerzoug[1,*] and F. Delaunois[2]

[1]Department of Mechanical Engineering, University of Biskra, B.P.145, 07000, Biskra, Algeria
[2]Metallurgy Department, University of Mons, 7000, Mons, Belgium

ABSTRACT – The aim of this investigation is to study the effect of time and temperature on the solid-state diffusion welding of commercial aluminum alloy 2xxx series with a pure copper at 425°C, 475°C, 500°C, and 525°C during holding times from 15 min to 240 min. The main characterization techniques were optical microscopy, scanning electron microscopy, energy dispersive spectrometry, nanoindentation, microhardness measurements, and x-ray diffraction. Results showed that increasing the temperature and the holding time had an effect on the apparition of the intermetallics at the Al alloy/Cu interface. Five intermetallic phases namely Al2Cu, AlCu, Al3Cu4, Al2Cu3, and Al4Cu9 were identified at the interface. The mechanical properties of the welded joint Al/Cu alloy varied also with the time and temperature. The nanoindentation measurements showed that the highest values of hardness were recorded in AlCu and Al3Cu4 phases. The welding success of these dissimilar metals can be used for battery cables or to form heat exchanger plates for vehicles.

ARTICLE HISTORY
Received: 28th Dec 2021
Revised: 1st April 2022
Accepted: 24th June 2022
Published: 28th June 2022

KEYWORDS
Diffusion welding;
Aluminum alloy;
Copper;
Intermetallics;
Mechanical properties

INTRODUCTION

Dissimilar welding of metals is widely used in many industries since it provides safe structures with a combination of high mechanical properties and good cost [1]. Bimetals have been largely used in industry due to their good physical, chemical and mechanical properties, that cannot be obtained from a single material [2], [3]. Welding of dissimilar metals in order to reach a high strength and durable joints is a reasonable challenge for industrial applications[4]. This can be done by using various methods, from fusion welding to diffusion bonding. From these bimetal materials, copper and aluminum joints have been studied and used in the last few decades [5]–[7].

Dissimilar welding of aluminum (Al) and copper (Cu) is largely used in the electric power, electronic and piping industries [1]. Many research works have investigated dissimilar joints of Al-Cu made by solid-state welding and fusion welding processes in order to optimize their properties and strength [1].Al-Cu joints made by a fusion welding process lead to the apparition of brittle intermetallic compounds (IMCs), which cause failure during cooling[4]. Furthermore, it was reported that the increase in electrical resistivity of the Al/Cu joints is associated with the formation of IMCs, which act as an additional heat source during the transmission of electric current. Other than that, the presence of welding defects within the interface causes poor conductivity of the joints[8].

One of the benefits of the solid-state welding of Cu to Al is that it can reduce the formation and growth of interfacial IMCs by introducing severely plastic deformation and then reducing welding temperature and time. The main solid-state welding processes are friction welding [9]–[11], ultrasonic welding [12], explosive welding [13], cold roll welding [14], and diffusion bonding or diffusion welding [15]–[17], which is a solid-state welding process used for joining similar and dissimilar metals. This process is based on the principle of solid-state diffusion, wherein the atoms of two solids metallic surfaces intersperse themselves over time [18]. The main advantages of diffusion bonding are obtaining high-quality bonds, and the possibility of producing joints with low porosity and good continuity across the interface[19].

Many researchers investigated the interfacial bonding between Cu and Al. Uscinowicz [20] found that in Al−Cu bimetallic joint, the thickness of diffusion zone increases exponentially with increasing annealing temperature and annealing time[21]. He reported that the electrical resistivity of Cu/Al composites increases with increasing the intermetallic-layer thickness. These intermetallic compounds (IMCs), such as $CuAl_2$, CuAl, Cu_9Al_4, Cu_3Al_2 and Cu_3Al are inevitable during the welding process due to the high chemical affinity between copper and aluminum. To avoid the defects induced during solidification in the Al/Cu joint, the solid-state diffusion bonding is conducted below the eutectic temperature. However, long bonding time and high bonding pressure facilitate the growth of IMC [22]. For that reason, a thin layer of IMCs enhances the metallurgical bonding due to interface reaction [23], [24]. Nevertheless, a thick layer of IMCs (higher than 2.5 μm) decreases the mechanical and electrical properties of the joint [25].

It is noticed that the most important research was focused on the IMC development in Al−Cu bimetallic joint. It is well known that five equilibrium IMCs such as Al_2Cu (θ), AlCu(η_2), Al_3Cu_4 (ζ_2), Al_2Cu_3 (δ) and Al_4Cu_9 (γ_2) phases could be formed by diffusion bonding between Al and Cu at temperatures near 500°C [26]. According to Chen and Hwang [27], the sequence of diffusion mechanism in Al−Cu bimetallic joint at temperature intervals between 300 and 500°C is as follows: saturated solid solution forms on Al-side, Al_2Cu was supposed to form first, followed by the apparition of

*CORRESPONDING AUTHOR | Z. Boumerzoug | ✉ z.boumerzoug@univ-biskra.dz

Al_4Cu_9, and additional IMCs such as AlCu and Al_3Cu_4. However, this sequence can change depending on two parameters, temperature and bonding time of Al−Cu bimetallic joint.

The present work aims (i) to shed light on the microstructural evolutions accompanying the Cu/Al alloy solid-state diffusion. (ii) to determine and discuss the thermokinetics parameters (n, k and Q) in the frame of the microstructural evolutions. (iii) to evaluate the micromechanical properties of the equilibrium phases (H and E). The solid-state diffusion process has been achieved at 425°C, 475°C, 500°C, and 525°C during holding times from 15 min to 240 min. The micromechanical and microstructural properties of the welded joint were carried out by using an optical microscope, a scanning electron microscope equipped with energy-dispersive spectroscopy (EDS), hardness, and nanoindentation measurements.

EXPERIMENTAL PROCEDURE

The two base metals used in this study were commercial aluminum alloy 2xxx series and high purity copper. Table 1 shows the chemical composition of the two base metals used in the present study.

Table 1. Chemical composition of aluminum alloy and copper used in diffusion welding.

Element (wt. %)	Al	Si	Cu	Zn	Cr	Pb	Ni
Al 2xxx	Bal	0.598	5.610	0.070	0.023	0.05	0.025
Copper	0.067	0.006	Bal	0.1	0.014	0.018	0.013

Samples of dimensions 50× 10×50 mm were cut and prepared. After cutting, mechanical polishing was carried out on emery papers with grain sizes of 600, 800, 1200, and 2400. The mechanical polishing was followed by chemical pickling. The pickling solution used for copper was composed of 15% H_2SO_4, 15% HNO_3, and 10% HCl, the one used for the aluminum alloy consisted of 10% NaOH followed by immersion in a solution of 50% HNO_3. A rinsing with ethanol and ultrasonic cleaning were applied after chemical stripping in order to remove oxides and impurities from the surface.

As shown in Figure 1**,** the samples were then superimposed in a support (copper at the bottom) equipped with a tightening screw to exert a homogeneous pressure. The pressure exerted was adjusted using a torque wrench. It is noted that the pressure was kept constant for each manipulation. The samples were then heated (at a constant speed of 4 °C/min) in a THERMOCONCEPT brand furnace from room temperature to the different welding temperatures T (425°C, 475°C, 500°C, and525°C). They were then maintained for different welding times, t, (of 15 min , 30 min, 60 min, 120 min and 240 min) under an argon/helium controlled atmosphere. Finally, the welded joints underwent ambient air cooling (air quenching).

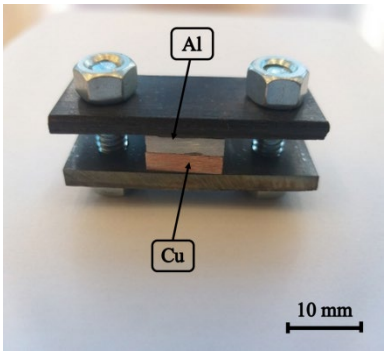

Figure 1. Diffusion bonding setup for joining aluminum alloy to copper.

Once the welded samples were removed from the support, they were cut perpendicular to the joining surface (interface) using electro-discharge machining (EDM) and mechanically polished on SiC-based papers with an increasing particle size from 600 to 4000. A finishing sheet with two suspensions of 3 µm and 1 µm was applied, followed by a final polishing under OPS suspension.

The microstructural analysis of the interface was performed using a HIROX KH8700 brand optical microscope and a scanning electron microscope (Zeiss Gemini SEM300) equipped with an EDS and BSE detectors for the local chemical analysis and phase images. The phase identification in the Al-Cu joint interface was made by using the x-ray diffraction performed on a Bruker D-5000 diffractometer, with $Cu_{K\alpha}$ radiation (1.5406 Å) as a source for phase identification, in 2θ range from 15 to 90°. Microhardness measurements were made at the interface using an HM-200 microdurometer under an applied load of 50gf. Nanoindentation measurements were conducted using an Anton PaarTritec SA nanoindenter, on the different IMC phases in order to evaluate their hardness and Young's modulus values using Oliver and Pharr method [28]. The maximum load was fixed at 20 mN, and the loading and unloading rates at 40 mN/min. All the indentations were taken in the middle of the IMC phases in order to avoid their influence upon one another. Furthermore, indentation spacing has been considered to avoid any overlapping effect of neighboring indentations.

RESULTS AND DISCUSSION

Microstructures Evolution in the Interface of Al alloy/Cu Joint

Figure 2 presents the microstructural evolutions of the cross-section of the bonded two dissimilar metals Al alloy/Cu at different temperatures and at different holding times. It is observed that for low temperatures (450 and 475 °C), the intermetallic layers took 30 min to form. Two discontinuous Al-Cu IMC appeared near the interface and inside the aluminum side. On the other hand, for high temperatures (500 and 525 °C), the formation of the first intermetallic layers was triggered after only a holding time of 15 min, which shows the primordial effect of the temperature in the solid-state welding of these dissimilar metals. According to Kharchenko [29], the incubation time for the appearance of intermetallics in the Al-Cu interface is a few seconds at 500°C. It has been found that the thickness of layers in dissimilar Al/Cu joint increases with increasing operating temperature [30]. The number of intermetallic layers increases with the prolongation of the holding time, and these layers become almost continuous throughout the interface. The intermetallic layer thickness was found to be uniform throughout the cross-section of the joint with the appearance of a new yellowish fine layer.

This last observation confirms the literature data for diffusion of copper and aluminum, which mentioned a higher diffusion rate of copper in aluminum [4]. It is known that the maximum solubility of Cu in Al for a solid solution is only 5.65 wt. % [31]. In addition, some limited number of micro-voids (black) are also observed at the Al alloy-Cu joint. This phenomenon is due to the different inherent diffusion coefficients of chemical species, which facilitate the formation of Kirkendall voids at the interfaces of the base metals[32]. Diffusion at the Al / Cu interface is manifested by the inter-diffusion of the two base metals, that is, the diffusion of copper into aluminum and vice versa. Atomic diffusion at solid state follows Fick's law and the diffusion coefficient is expressed by an Arrhenius law [33]:

$$D = D_0 \cdot \exp\left(-\frac{Q}{RT}\right) \quad (1)$$

Where D_0 is the pre-exponential factor, R is the gas constant, T is the temperature, and Q is the activation energy of the diffusion. Table 2 shows the values of D_0 and Q in the case of solid-state inter diffusion of Al and Cu in the temperature range of 706-925 °K.

Table 2. Values of D_0 and Q for the inter-diffusion between Al and Cu [34]

	D_0 (cm^2/s)	Q (kJ)
Diffusion of Al in Cu	0.131	185.2
Diffusion of Cu in Al	0.647	135.1

The diffusion coefficient can be calculated for each temperature by replacing the values in Table 2 in the diffusion coefficient equation, the values calculated in our case are shown in Table 3. It is obviously noticed that the two diffusion coefficients $D_{Al\text{-}Cu}$ and $D_{Cu\text{-}Al}$ increase with increasing temperature since the diffusion phenomenon is thermally activated. In addition, the diffusion coefficient of Cu in Al ($D_{Cu\text{-}Al}$) is about four orders of magnitude larger than that of Al in Cu ($D_{Al\text{-}Cu}$), which implies that the diffusion in the solid-state of copper atoms into aluminum is much faster than that of aluminum towards copper. This could explain the appearance of new phases in the aluminum side of the Al / Cu interface. It has been reported that at a higher annealing temperature, the diffusion of copper becomes faster. Thus, more compounds or solid solutions could be easily formed[35]. Zhang et al. [36] also mentioned that inter-diffusion of atoms through the interface was promoted with a higher temperature annealing and a much thicker Al-Cu diffusion layer was obtained. They also reported that dislocations strongly controlled diffusional processes leading to the growth of IMCs.

Table 3. Values of the two diffusion coefficients $D_{Al\text{-}Cu}$ and $D_{Cu\text{-}Al}$ at different diffusion temperatures ($D_{Cu\text{-}Al}$: diffusion coefficient of Cu in Al, $D_{Al\text{-}Cu}$: diffusion coefficient of Al in Cu)

Temperature (°C)	$D_{Cu\text{-}Al}$ (m^2/s)	$D_{Al\text{-}Cu}$ (m^2/s)
450	$1{,}12 \cdot 10^{-14}$	$5{,}45 \cdot 10^{-19}$
475	$2{,}39 \cdot 10^{-14}$	$1{,}52 \cdot 10^{-18}$
500	$4{,}80 \cdot 10^{-14}$	$4 \cdot 10^{-18}$
525	$9{,}28 \cdot 10^{-14}$	$9{,}86 \cdot 10^{-18}$

In addition to the intermetallic layers, the formation of a eutectic layer was observed in Al side for the welded joints at 525 °C. This eutectic layer appeared just after a holding for 30 min and grew rapidly with the increase of the holding time. Zhou et al. [37] revealed that the weld zone of the Al/Cu joint primarily consists of α-Al solid solution and coral-like shaped Al–Cu eutectic phase. These microstructural observations indicate the effect of temperature and time bonding on the intermetallic layers types and thickness. Shen et al. [38] mentioned that the atomic migration of chemical species across interfaces (base metals) directly increased with increasing the temperature and time. Hua et al. [39] also reported that an increase in the diffusion area was enhanced by increasing the bonding temperature and time.

According to the Aluminum-Copper binary phase diagram (in Figure 3), several Al/Cu intermetallic phases, which include $Al_2Cu(\theta)$, $AlCu(\eta)$, $Al_3Cu_4(\zeta)$, $Al_2Cu_3(\delta)$ and $Al_4Cu_9(\gamma)$ may develop during solid-state diffusion bonding. In order to identify these phases, XRD and EDS analyses were conducted.

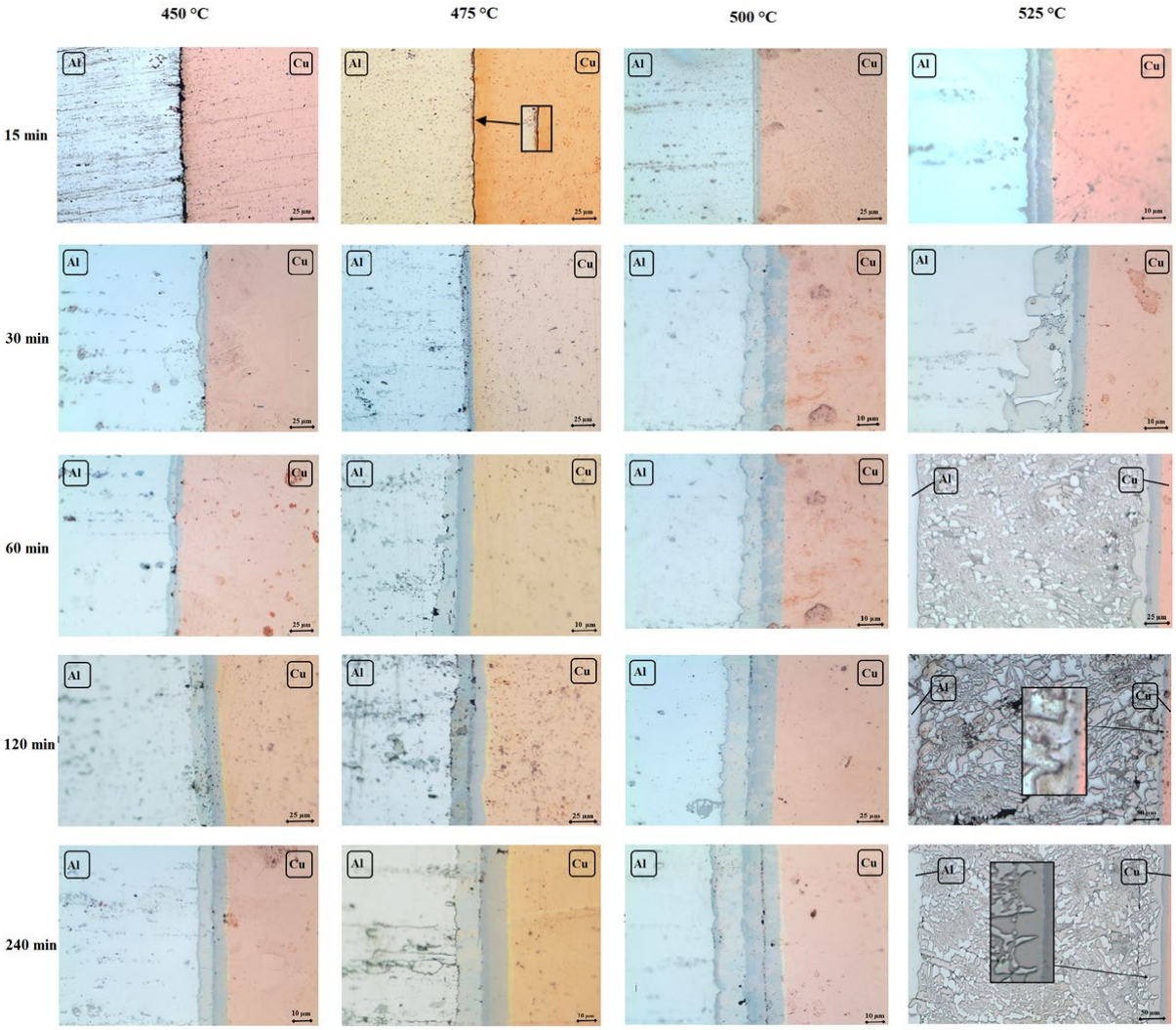

Figure 2. Microstructures evolution of the bonded Al alloy/Cu joint at different temperatures and holding time.

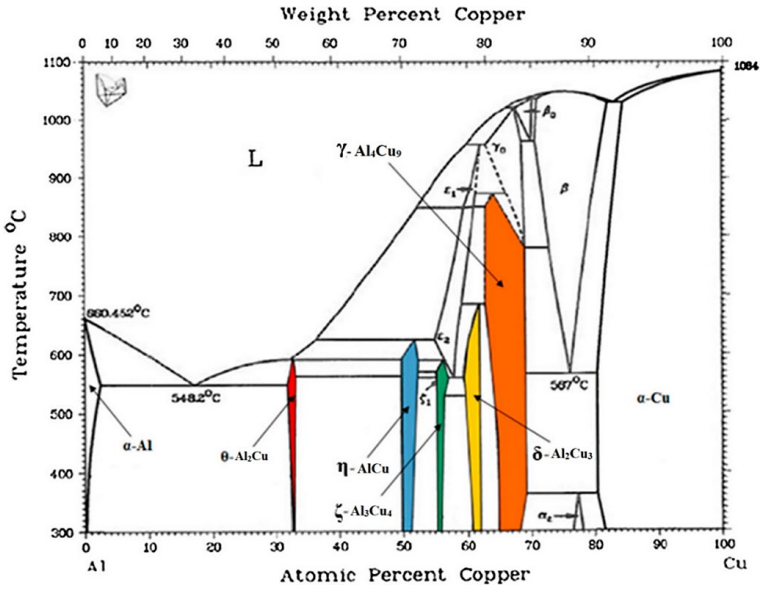

Figure 3. Al-Cu binary phase diagram [40].

XRD Analysis

Figure 4 to Figure 7 show the XRD diffractograms of Al alloy/Cu welded joints at the four temperatures studied in the present work. Only the diffractograms obtained from the initial (15 min) and final states (240 min) of diffusion welding were selected. For the temperature of 450°C (in Figure 4) and holding time of 15 min, only the peaks of three phases were

revealed, namely aluminum and copper, which are the phases of the base metals, as well as Al_2Cu, which coexists in Al as a precipitate in the aluminum matrix. Other weak peaks appear in the X-ray diffractogram when increasing the welding time to 240 min. These peaks correspond to the following phases: Al_3Cu_4, AlCu, Al_2Cu, Al_2Cu_3, and Al_4Cu_9. It is finally noted the appearance of only one peak for each phase.

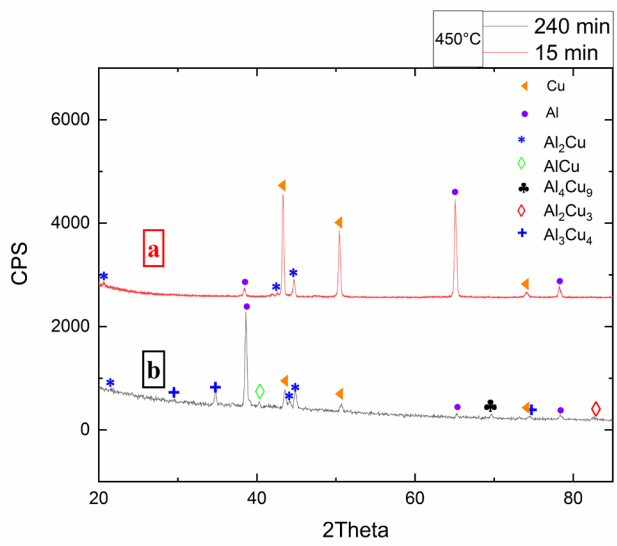

Figure 4. X-ray diffractogram of the Al alloy/Cu joint welded at 450°C for (a) 15 min, and (b) 240 min

It is worth noticing that when samples were held at 500 ° C for 15 min (in Figure 6), the intermetallic phase peaks remain weakly detectable by X-ray, and only AlCu and Al_3Cu_4 were detected. However, when the holding time is 240 min, the peaks of the various intermetallic phases are more intense and more numerous, which confirms the formation of these IMC phases at the Al alloy/Cu interface as observed by optical microscopy.

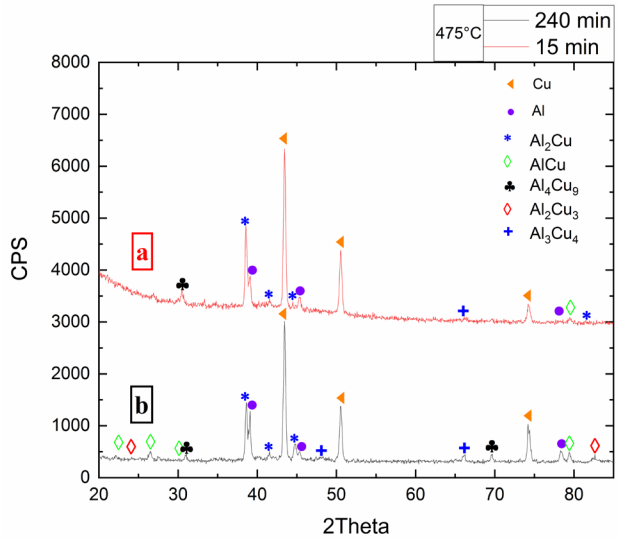

Figure 5. X-ray diffractogram of the Al alloy/Cu joint welded at 475°C for (a) 15 min, and (b) 240 min

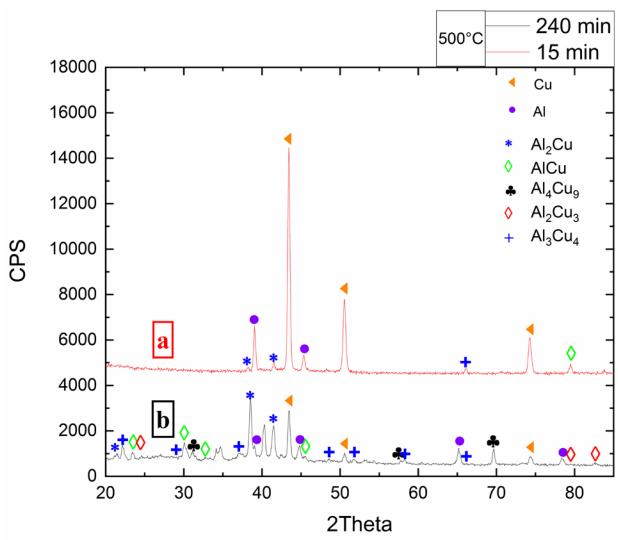

Figure 6. X-ray diffractogram of the Al alloy/Cu joint welded at 500°C for (a) :15 min, and (b) : 240 min.

For the highest holding temperature (525 °C) (in Figure 7) and despite the short holding time of 15 min, the peaks of the five intermetallic phases mentioned above were well detected. It is noticed that increasing the holding time to 240 min led to a decrease in the peaks intensity, except for the Al_2Cu phase. This could be explained by considering that at these conditions of temperature and time, the dominant reaction is the shrinkage of the IMCs at the interface, which favors the apparition of the Al + Al_2Cu eutectic phase. It is important to mention that the variation in intensities of the detected peaks may be attributed to the presence of crystallographic texture.

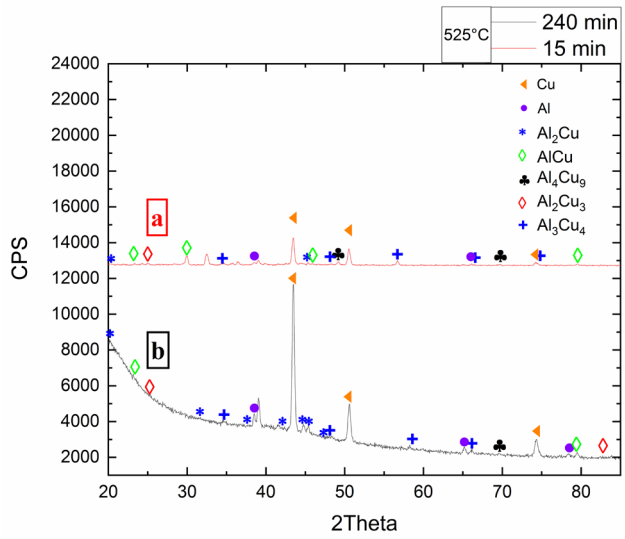

Figure 7. X-ray diffractogram of the Al alloy/Cu joint welded at 525°C for (a) 15 min, and (b) 240 min.

EDS Analysis

An EDS analysis was performed to study the exact composition of each IMC layer. For that reason, as shown in Figure 8, a selected zone was chosen from the Al alloy/Cu welded joint heated at 450°C for 240 min. It is noticed from Figure 8(a), that four distinct phases were formed between Al alloy and Cu. These phases are sandwiched and parallel to the interface with different thicknesses as indicated by (1), (2), (3) and (4). The first three phases have different contrast of grey from aluminum alloy side to copper side, whereas the forth one exhibits a yellowish color.

In order to have more details concerning the Al alloy/Cu interface, the backscattered electrons BSE image of the interface was used (Figure 8(b)). Five alternating bright and dark regions are observed, which are indicative of the intermetallic layers in the Al alloy/Cu interface, as mentioned by Xiao et al. [41] and Galvão et al. [42]. This conclusion is based on the relative contrast, which in turn, is related to the relative level of copper and aluminum in the intermetallic phases. Region (2) in Figure 8(a) is actually composed of two different phases, as confirmed in Figure 8(b). Despite the good resolution of the SEM image, the region (4) previously observed with optical microscope, is almost undetectable. It is worth noticing that seven points were chosen to perform a local chemical analysis. The results of the EDS analysis (Table 4) showed that five intermetallic phases from Al alloy side to copper side are detected: Al_2Cu, AlCu, Al_3Cu_4, Al_2Cu_3 and Al_4Cu_9. This last result is in agreement with a previous study reported by Bergmann et al. [4].

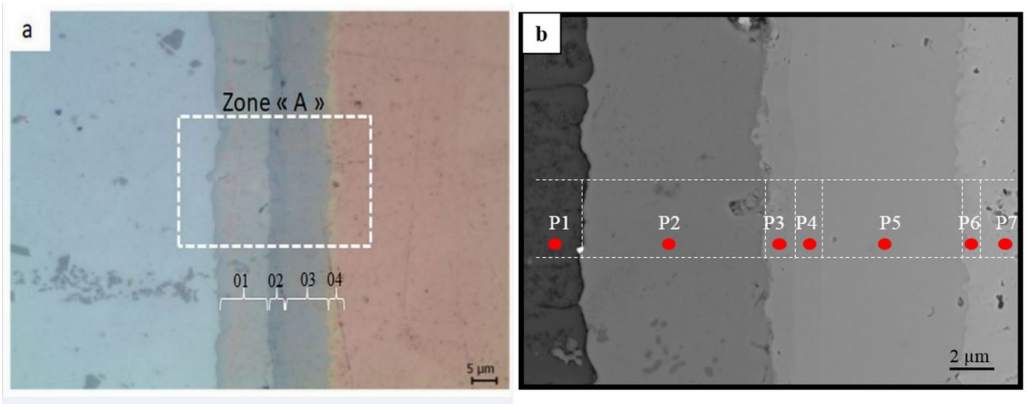

Figure 8. (a) Micrograph and (b): BSE image of Al alloy/Cu joint welded at 450°C for 240.min.

Table 4. Punctual EDS analysis of Al alloy/Cu joint Welded at 450°C for 240 min.

Position	Atomic fraction (%)		Error (±%)	Possible phase
	Al	Cu		
P1	97.91	2.09	2.05	Al
P2	66.62	33.38	2.03	Al_2Cu
P3	49.01	50.99	2.34	AlCu
P4	43.94	56.06	2.22	Al_3Cu_4
P5	39.76	60.24	2.20	Al_2Cu_3
P6	28.91	71.09	2.17	Al_4Cu_9
P7	0.35	99.65	2.15	Cu

Kinetics of IMCs Phases Precipitation

In order to assess the effect of temperature and dwelling time on the Evolution of the diffusion layer, relative thicknesses of IMCs were calculated by dividing the IMC thickness by the whole diffusion layer thickness. It is noticed that the increase of the dwelling time appear to favor the expansion of Al_3Cu_4 and Al_4Cu_9 to the detriment of Al_2Cu_3, AlCu and Al_2Cu. As mentioned by Chen and Hwang [27], the thicknesses of AlCu and Al_3Cu_4 were measured together due to the difficulty of differentiating these two phases at low temperature (of 450°C). However, a higher temperature favors the Al_2Cu and Al_2Cu_3 growth to the detriment of the rest of IMCs. This suggests that both dwelling time and temperature contribute to the growth kinetics of IMC, though only the bonding temperature has a more important effect on their formation. Based on the classical kinetic theory, the mathematical relationship between the thickness of the developed layer (y) and the time (t) at a given temperature can be expressed by the following equation [42]:

$$y = kt^n \tag{2}$$

Where k is the growth rate constant and n is the time t exponent. A linear growth is obtained in case the growth rate is limited by the reaction rate at the growth site. However, parabolic growth is expected when the growth process is controlled by volume diffusion. The average thicknesses of intermetallic layers observed in the Al alloy/Cu joint are plotted in Figure 9. The growth rate constant was calculated from a regression analysis of y versus t^n [21]. For these intermetallic layers (Al_2Cu, Al_2Cu_3, AlCu+Al_3Cu_4), the curves shape is parabolic, which suggests that their growth is controlled by volume diffusion.

A simple mathematical development of Eq. (2) permitted us to evaluate n and k parameters. A simple Arrhenius equation was applied to determine the activation energies of the intermetallic compounds growth [43]:

$$k = k_0 \exp\left(-\frac{Q}{RT}\right) \tag{3}$$

Where k_0 is the frequency factor, Q is the activation energy, R is the gas constant (8.314 J/mol.K) and T is the welding temperature. Figure 10 presents the Napierian logarithms plots versus reciprocal of T ($1/T$) for the growth of Al_2Cu, AlCu+Al_3Cu_4, Al_2Cu_3 and Al_4Cu_9 intermetallic layers. The activation energy was calculated from the slope of the Arrhenius plot using linear regression. Values of n, k and Q are summarized in Table 5.

Table 5. Calculated thermokinetics parameters (n, k and Q).

IMCs Phases	n	k (s^{-1})	Q (kJ/mol)
Al2Cu	0.45	2.34	131.7
Al2Cu3	0.41	1.94	119.7
AlCu+Al3Cu4	0.4	1.81	141.1
Al4Cu9	0.47	0.5	243.1

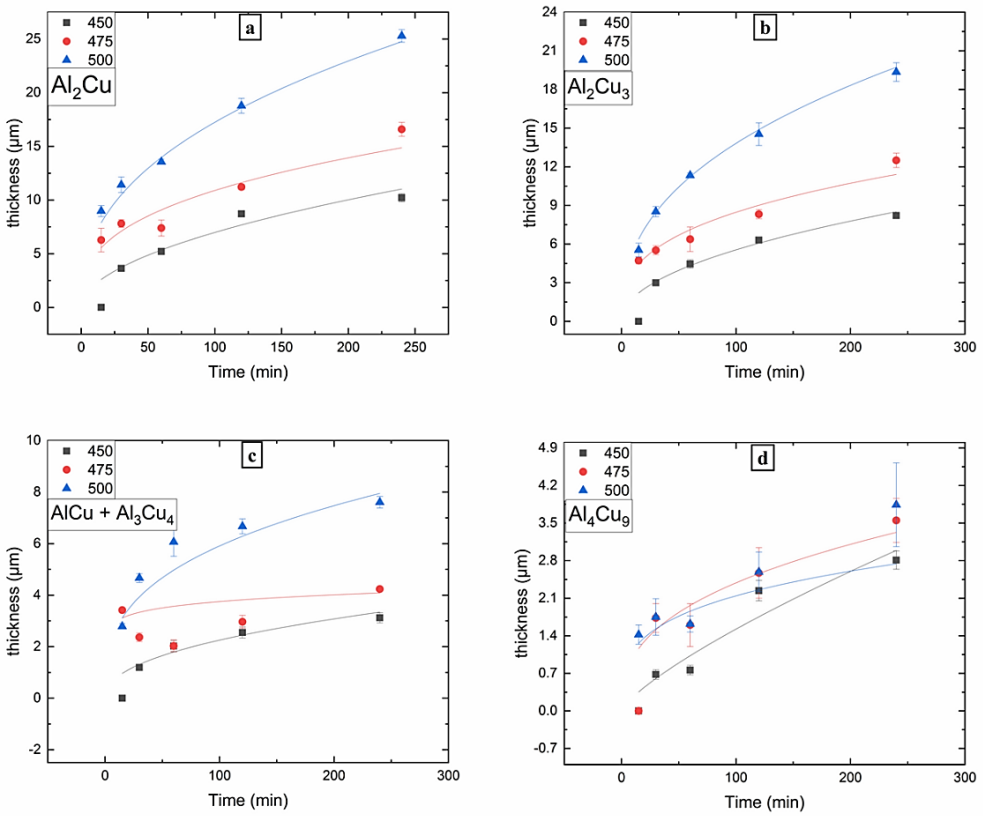

Figure 9. Thickness variation of different layers of the bonded Al-Cu versus holding time: (a) Al_2Cu, (b) Al_2Cu_3, (c) $AlCu+Al_3Cu_4$ and (d) Al_4Cu_9

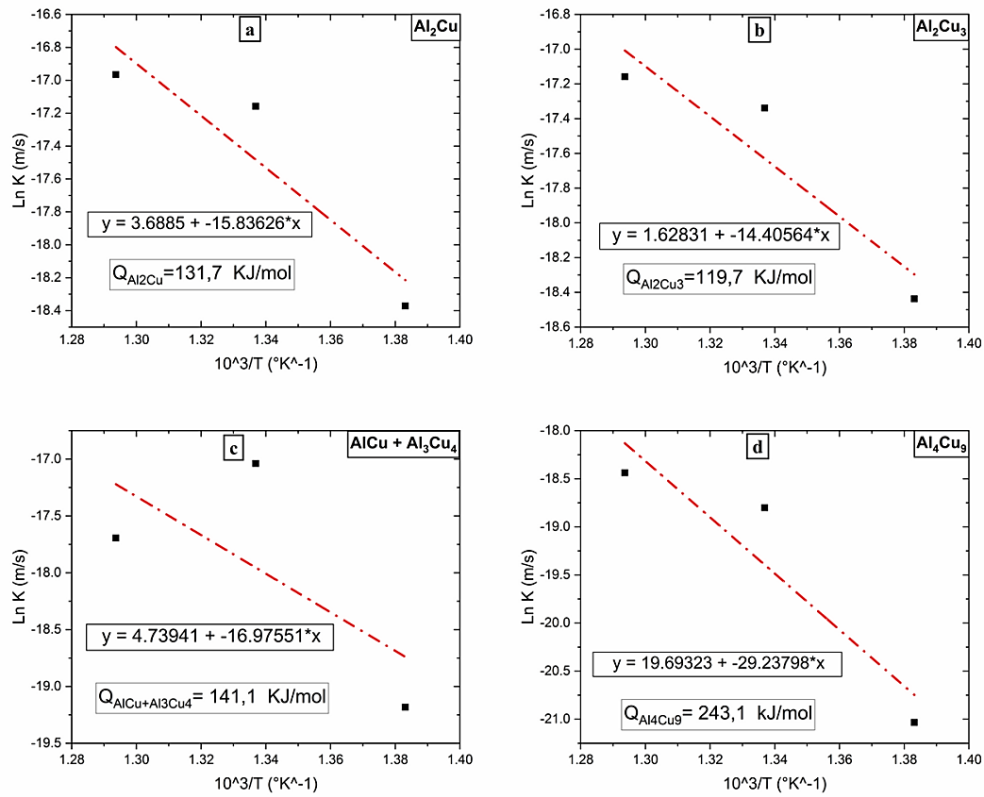

Figure 10. Napierian logarithms plots versus reciprocal of T ($1/T$): (a) Al_2Cu, (b) Al_2Cu_3, (c) $AlCu+Al_3Cu_4$ and (d) Al_4Cu_9

It is noticed from Table 5 that an almost unique value of n is obtained for all the IMCs studied phases (n = 0.43). According to Gil et al. [43], $n < 0.5$ corresponds to normal growth. Besides, the highest value of k is recorded for the

Al_2Cu phase, whereas the lowest one is obtained for Al_4Cu_9 phase. On the other hand, values of Q of the Al_2Cu, Al_2Cu_3 and $AlCu+Al_3Cu_4$ phases are close to the activation energy of the Cu diffusion in Al except for Al_4Cu_9, which exhibits the largest Q value. This could be explained by considering that the formation of this phase is accompanied by the interdiffusion of Al and Cu across the interface.

Based on the microstructural observations, x-ray difffraction, EDS analysis and thermokinetics investigation (values of the rate constant k), it can be suggested that the sequence of the intermetallic layers precipitation in Al alloy/Cu interface (Figure 11(a)) occurred as follows: Al_2Cu and Al_2Cu_3 layers were formed first in solid solution of the Al alloy (Figure 11 (b)), followed by the formation of the two layers AlCu and Al_3Cu_4 (Figure 11 (c)). Finally, the Al_4Cu_9 layer appeared as in Figure 11(d).

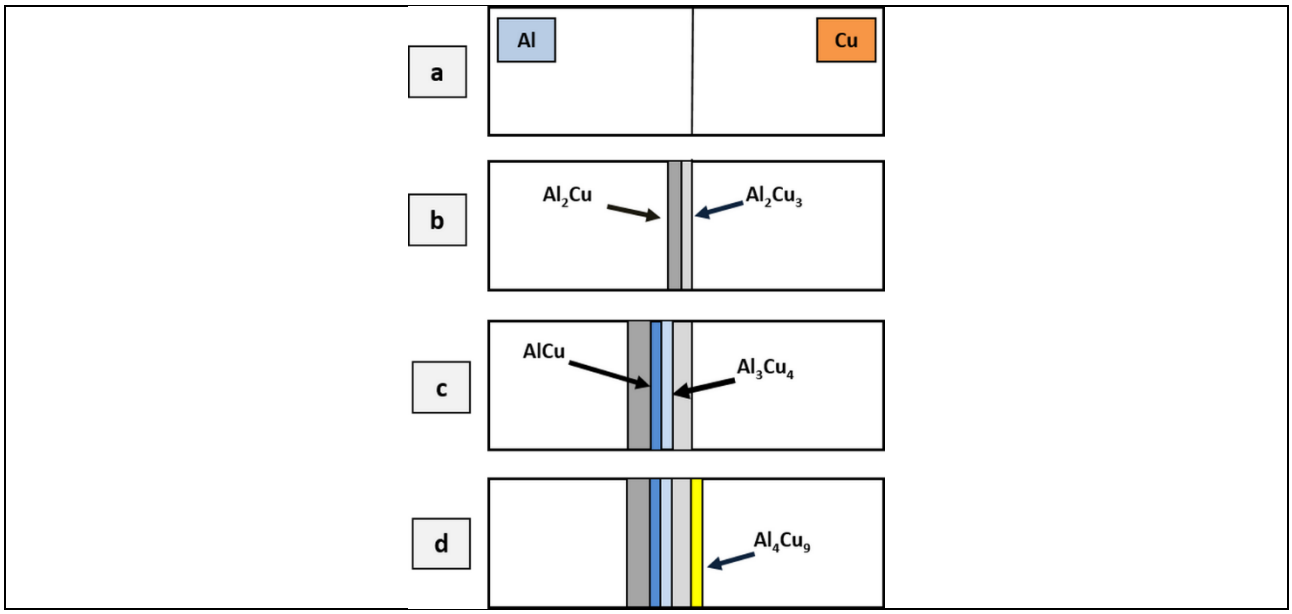

Figure 11. Schematic representation of the sequence of occurrence of intermetallic layers in Al alloy/Cu joint (a) Al/Cu (b) apparition of Al_2Cu and Al_2Cu_3 (c) apparition of AlCu and Al_3Cu_4 (d) apparition of Al_4Cu_9.

Hardness Measurement

Figure 12 shows the development of microhardness of the welded joints at different temperatures and holding times. As shown in Figure 12(a), the microhardness values on the aluminum side were higher than those recorded on the copper side. The microhardness of aluminum is in the order of 112 Hv, that of copper is 56 Hv, and no change was observed in the microhardness of the two base metals for all welded joints. In addition, the microhardness of the interdiffusion zone displays higher values than those of aluminum or copper base metals, confirming both the interdiffusion of the main elements and the formation of Al-Cu intermetallic compounds.

It can be also concluded that the microhardness profile across the welded joint depends on the temperature and the holding time. It is noticed that at low temperature (450°C) and for short welding times (15 and 30 min), a slight increase of microhardness at the Al alloy/Cu interface. This is due either to the absence or to the very low interdiffusion in Al alloy/Cu interface. By increasing the holding time up to 60 and 120 min, high microhardness values were measured because the indenter touches the two layers (Al_2Cu and Al_2Cu_3), which exhibit high microhardness values. A microhardness peak of 536 Hv was obtained for the welded joint during 240 min. This highest microhardness value is due to the growth of IMCs, namely the two middle layers (AlCu and Al_3Cu_4), which are the hardstone.

At 475°C and for a holding time of 15 min, the microhardness at the interface is relatively high due to the presence of thin and discontinuous intermetallics. However, the higher the holding time, the higher the thickness of the IMCs and, consequently, the greater the microhardness. The greatest microhardness values were measured at 30 and 240 min, which correspond to the indentations in the middle of the IMCs.

At 500 °C, it is observed that the welded joints have wider interfaces with respect to the welded joints at 450 and 475°C. At high temperatures, the driving force for the migration of Al and Cu atoms increases, which promotes the development of a larger interdiffusion zone, and, thus, the formation of IMC. The microhardness at the interface corresponds only to the intermetallics and varies between 470 and 580 Hv. This variation is linked to the position of the indenter, which often touches the interface between two IMCS. The maximum measured value is 732 Hv, which corresponds to the microhardness of the two intermediate layers namely AlCu and Al_3Cu_4.

For the welding at 525 °C, the curve can be divided into two intervals. The first one corresponds to the microhardness measurements recorded at the level of the IMCs; its width is small because at this temperature, the IMCs start to decrease and the main reaction occurring during welding is the formation of the eutectic phase ($Al + Al_2Cu$). The second interval, which takes the form of a plateau with an average value of 250 Hv, characteristic of the eutectic layer.

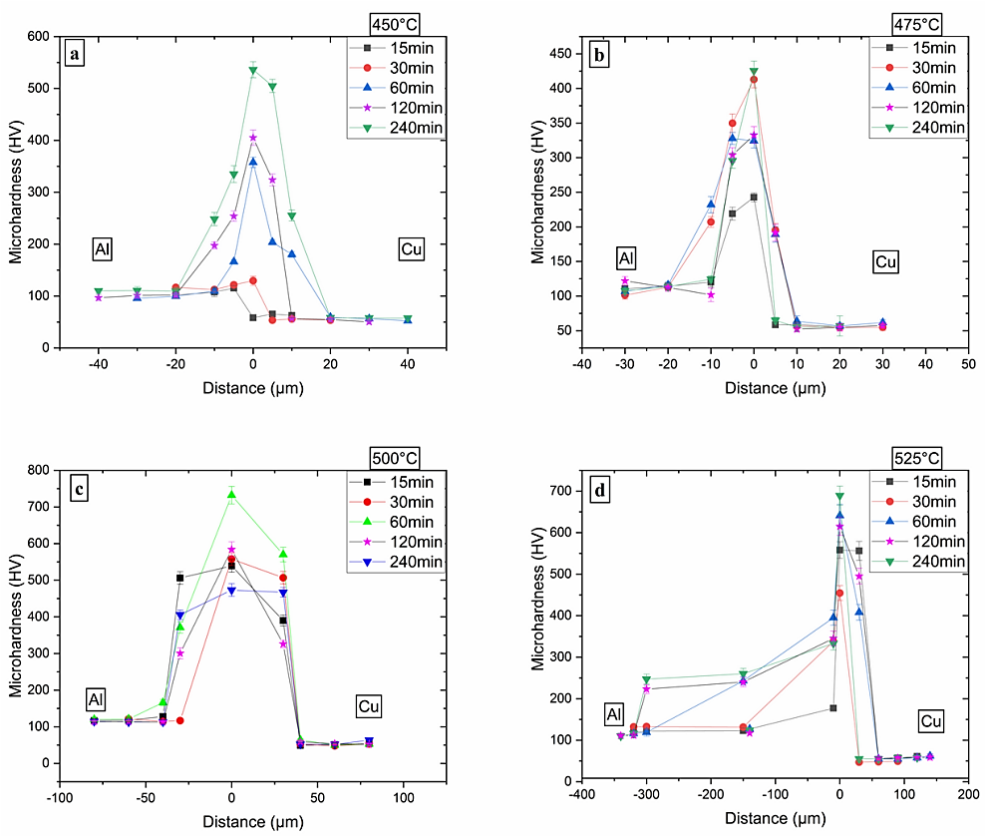

Figure 12. Microhardness profiles of the bonded Al alloy/Cu at (a) : 450 °C, (b) : 475°C, (c) : 500°C, and (d) : 525°C

Nanoindentation Tests

The load-displacement (*P-h*) curves issued from nanoindentation tests performed on each IMC phase are depicted in Figure 13. Three distinguished set curves can be observed with respect to the penetration depth: the first one corresponds to the Al_2Cu intermetallic with the highest depth values. The second one corresponds to the curves with similar displacement depth that are attributed to Al_3Cu_4 and AlCu IMC phases and the third set with intermediate depth values, corresponds to Al_2Cu_3 phase.

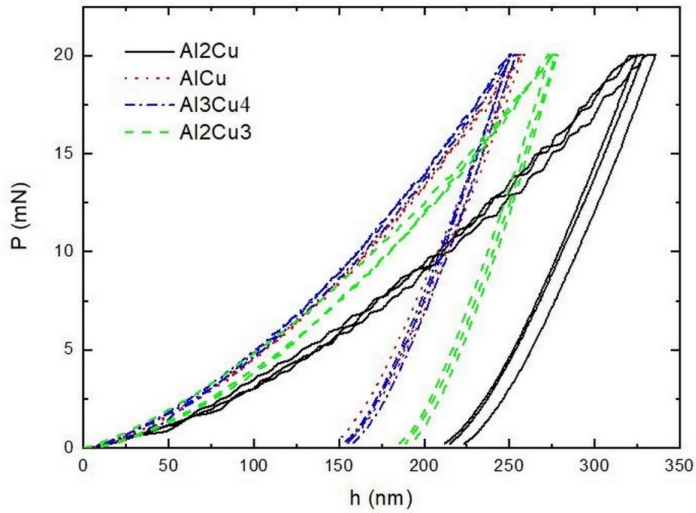

Figure 13. Nanoindentation charge versus the displacement on the individual IMC phases of Al alloy/Cu joint welded at 500°C for 240 min.

The maximum penetration depth at the end of loading segment suggested that the AlCu and Al_3Cu_4 IMCs are mechanically harder than the other IMC phases, which is in good agreement with the results reported by Bergmann et al. [4]. On the other side, the slope in the unloading segment is slightly steeper in the AlCu and Al_3Cu_4 than in Al_2Cu IMCs, reflecting the high stiffness values of the former.

The microhardness (H_{IT}) and elastic modulus (E_{IT}) values of the different phases, estimated using the Oliver and Pharr method [28], are summarized in Figure 14(a) and (b). It can be noticed that all the IMC phases exhibit high H_{IT} and E_{IT}

values compared to base metals (Al and Cu). The highest values were recorded in AlCu and Al_3Cu_4 phases with 20.32GPa and 19.63 GPa for the microhardness and 227.5 GPa and 256.3 GPa for the elastic modulus, respectively. As mentioned above, the lowest microhardness and young's modulus values were recorded in Al_2Cu phase with 10.9 GPa and 153.6 GPa, respectively. This behavior can be explained by considering dislocation mobility. Indeed, as reported by Xiao et al. [40], crystal structures with low symmetry exhibit low dislocations mobility and consequently high microhardness values. Thus, AlCu and Al3Cu4 phases with monoclinic and orthorhombic crystal structures respectively present the highest microhardness values.

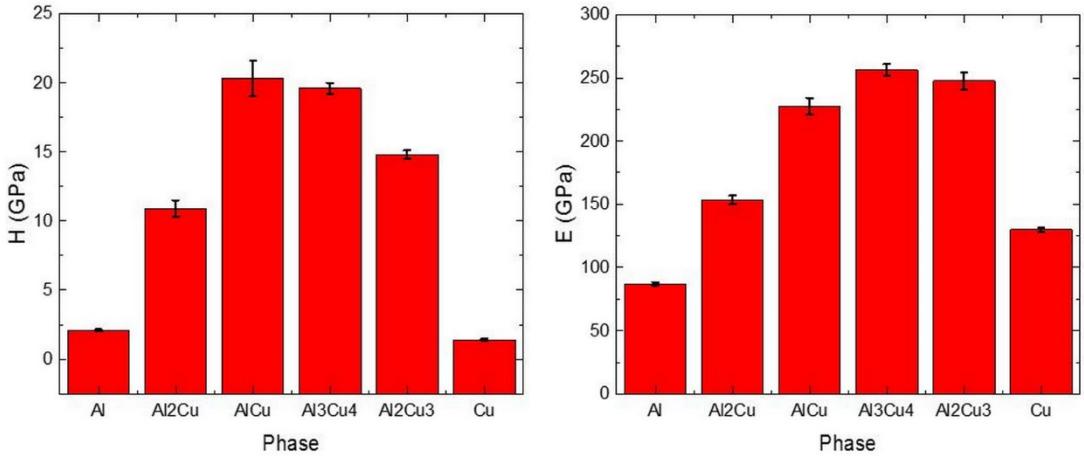

Figure 14. Nanohardness (H) and Young's modulus (E) of each phase of Al alloy/Cu joint welded at 500°C for 240 min.

CONCLUSION

In summary, the present study is a contribution to study the joining of aluminum alloy with copper via solid-state diffusion process. The effect of time and temperature during the joining process was studied. The main results obtained in the present work can be summarized as follows:

i. Aluminum alloy and copper were successfully joined by solid state diffusion welding process.
ii. The main transformations were observed on the Al side since the different intermetallic layers were formed within.
iii. Increasing the temperature and time during the diffusion bonding leads to the apparition of different types of intermetallic compounds whose thicknesses increase consequently.
iv. Five intermetallic phases from Al side to copper are distinguished: Al_2Cu, AlCu, Al_3Cu_4, Al_2Cu_3, and Al_4Cu_9.
v. At higher bonding temperature (525°C), only the third layer underwent a morphological transformation by growth reaction in Al side and development of a eutectic structure.
vi. Thermokinetics parameters (n, k and Q) have been calculated. A unique value of n =0.43 has been obtained, suggesting a normal growth of the IMCs phases. Besides, the higher value of k (which stands for the fastest growth kinetics) corresponds to the growth of Al_2Cu. This is consistent with the microstructural evolutions.
vii. The growth activation energy of Al_4Cu_9 is the highest among the IMCs
viii. The higher the bonding temperature, the higher the microhardness of the interdiffusion zone because the latter exhibits considerably higher values of microhardness than those recorded in the base metals.
ix. The nanoindentation measurements showed that the highest values of hardness were recorded in AlCu and Al_3Cu_4 phases with 20.32 GPa and 19.63 GPa.

ACKNOWLEDGEMENT

The authors would like to thank WBI and MESRS of Algeria for their financial support. We also thank the entire team of the metallurgy department of the University of Mons for their technical support and encouragement.

REFERENCES

[1] M. S. M. Isa *et al.*, "Recent research progress in friction stir welding of aluminium and copper dissimilar joint: a review," *J. Mater. Res. Technol.*, vol. 15, pp. 2735–2780, 2021, doi: 10.1016/j.jmrt.2021.09.037.
[2] N. Chen *et al.*, "Microstructural characteristics and crack formation in additively manufactured bimetal material of 316L stainless steel and Inconel 625," *Addit. Manuf.*, vol. 32, no. September 2019, 2020, doi: 10.1016/j.addma.2020.101037.
[3] Q. Hu, X. Wang, X. Shen, and Z. Tan, "Microstructure and corrosion resistance in bimetal materials of Q345 and 308 steel wire-arc additive manufacturing," *Crystals*, vol. 11, no. 11, 2021, doi: 10.3390/cryst11111401.
[4] J. P. Bergmann, F. Petzoldt, R. Schürer, and S. Schneider, "Solid-state welding of aluminum to copper—case studies," *Weld. World*, vol. 57, no. 4, pp. 541–550, 2013, doi: 10.1007/s40194-013-0049-z.

[5] L. Fang, J. Huang, Y. Liu, B. Zhang, and H. Li, "Cored-wire arc spray fabrication of novel aluminium-copper coatings for anti-corrosion/fouling hybrid performances," *Surf. Coatings Technol.*, vol. 357, no. July 2018, pp. 794–801, 2019, doi: 10.1016/j.surfcoat.2018.10.094.

[6] J. K. Han *et al.*, "Direct bonding of aluminum–copper metals through high-pressure torsion processing," *Adv. Eng. Mater.*, vol. 20, no. 11, pp. 1–9, 2018, doi: 10.1002/adem.201800642.

[7] N. A. Muhammad and C. S. Wu, "Evaluation of capabilities of ultrasonic vibration on the surface, electrical and mechanical behaviours of aluminium to copper dissimilar friction stir welds," *Int. J. Mech. Sci.*, vol. 183, no. May, 2020, doi: 10.1016/j.ijmecsci.2020.105784.

[8] R. Khajeh *et al.*, "Microstructure, mechanical and electrical properties of dissimilar friction stir welded 2024 aluminum alloy and copper joints," *J. Mater. Res. Technol.*, vol. 14, pp. 1945–1957, 2021, doi: 10.1016/j.jmrt.2021.07.058.

[9] D. Wu, W. Li, X. Liu, Y. Gao, Q. Wen, and A. Vairis, "Effect of material configuration and welding parameter on weld formability and mechanical properties of bobbin tool friction stir welded Al-Cu and Al-Mg aluminum alloys," *Mater. Charact.*, vol. 182, no. July, 2021, doi: 10.1016/j.matchar.2021.111518.

[10] W. Hou *et al.*, "The role of tool offset on the microstructure and mechanical properties of Al/Cu friction stir welded joints," *J. Alloys Compd.*, vol. 825, p. 154045, 2020, doi: https://doi.org/10.1016/j.jallcom.2020.154045.

[11] G. Li *et al.*, "Influence of dwell time on microstructure evolution and mechanical properties of dissimilar friction stir spot welded aluminum-copper metals," *J. Mater. Res. Technol.*, vol. 8, no. 3, pp. 2613–2624, 2019, doi: 10.1016/j.jmrt.2019.02.015.

[12] S. Ao *et al.*, "Microstructure evolution and mechanical properties of Al/Cu ultrasonic spot welded joints during thermal processing," *J. Manuf. Process.*, vol. 41, no. 135, pp. 307–314, 2019, doi: 10.1016/j.jmapro.2019.04.006.

[13] M. K. G. Shiran *et al.*, "Multilayer Cu/Al/Cu explosive welded joints: Characterizing heat treatment effect on the interface microstructure and mechanical properties," *J. Manuf. Process.*, vol. 35, no. January, pp. 657–663, 2018, doi: 10.1016/j.jmapro.2018.09.014.

[14] J. Feng, "Texture development in the interfacial zone of Al/Cu bimetal cold roll-bonded for E-mobility," *Mater. Lett.*, vol. 236, pp. 139–143, 2019, doi: 10.1016/j.matlet.2018.10.079.

[15] M. Elsa, A. Khorram, O. O. Ojo, and M. Paidar, "Effect of bonding pressure on microstructure and mechanical properties of aluminium/copper diffusion-bonded joint," *Sadhana - Acad. Proc. Eng. Sci.*, vol. 44, no. 5, 2019, doi: 10.1007/s12046-019-1103-3.

[16] Q. Teng, X. Li, and Q. Wei, "Diffusion bonding of Al 6061 and Cu by hot isostatic pressing," *J. Wuhan Univ. Technol. Mater. Sci. Ed.*, vol. 35, no. 1, pp. 183–191, 2020, doi: 10.1007/s11595-020-2242-4.

[17] W. Melik, Z. Boumerzoug, and F. Delaunois, "Solide state diffusion bonding of Al6061-SiC nanocomposites," *Int. J. Automot. Mech. Eng.*, vol. 18, no. 4, pp. 9305–9311, 2021, doi: https://doi.org/10.15282/ijame.18.4.2021.13.0716.

[18] T. Violeta, L. Mariana, L. Lucia, and A. Georgeta, "Materials bonding by diffusion welding technology," *Innov. Technol. Join. Adv. Mater. Mater.*, no. June, pp. 1–6, 2007.

[19] A. H. Assari and B. Eghbali, "Solid state diffusion bonding characteristics at the interfaces of Ti and Al layers," *J. Alloys Compd.*, vol. 773, pp. 50–58, 2019, doi: 10.1016/j.jallcom.2018.09.253.

[20] R. Uscinowicz, "Impact of temperature on shear strength of single lap Al–Cu bimetallic joint," *Compos. Part B Eng.*, vol. 44, no. 1, pp. 344–356, 2013, doi: 10.1016/j.compositesb.2012.04.073.

[21] J. Zhang *et al.*, "Formation and growth of Cu–Al IMCs and their effect on electrical property of electroplated Cu/Al laminar composites," *Trans. Nonferrous Met. Soc. China*, vol. 26, no. 12, pp. 3283–3291, 2016, doi: 10.1016/S1003-6326(16)64462-X.

[22] J. Xiong *et al.*, "Microstructure and mechanical properties of Al-Cu joints diffusion-bonded with Ni or Ag interlayer," *Vacuum*, vol. 147, pp. 187–193, 2018, doi: 10.1016/j.vacuum.2017.10.033.

[23] M. J. Kim, K. S. Lee, S. H. Han, and S. I. Hong, "Interface strengthening of a roll-bonded two-ply Al/Cu sheet by short annealing," *Mater. Charact.*, vol. 174, no. March 2020, 2021, doi: 10.1016/j.matchar.2021.111021.

[24] H. Xu *et al.*, "New observation of nanoscale interfacial evolution in micro Cu–Al wire bonds by in-situ high resolution TEM study," *Scr. Mater.*, vol. 115, pp. 1–5, 2016, doi: 10.1016/j.scriptamat.2015.12.025.

[25] M. Braunovic, "Reliability of power connections," *J. Zhejiang Univ. Sci. A*, vol. 8, no. 3, pp. 343–356, 2007, doi: 10.1631/jzus.2007.A0343.

[26] H.-J. Kim *et al.*, "Effects of Cu/Al intermetallic compound (IMC) on copper wire and aluminum pad bondability," *IEEE Trans. Components Packag. Technol.*, vol. 26, no. 2, pp. 367–374, 2003, doi: 10.1109/TCAPT.2003.815121.

[27] C.-Y. Chen and W.-S. Hwang, "Effect of annealing on the interfacial structure of aluminum-copper joints," *Mater. Trans.*, vol. 48, no. 7, pp. 1938–1947, 2007, doi: 10.2320/matertrans.MER2006371.

[28] W. C. Oliver, and G. M. Pharr, "An improved technique for determining hardness and elastic modulus using load and displacement sensing indentation experiments" *Journal of Materials Research*, 7, pp. 1564-1583. 1992, https://doi.org/10.1557/JMR.1992.1564

[29] G.K. Kharchenko *et al.*, "Vacuum percussion welding of aluminium to copper," *Pat. Weld. J.*, vol. 46, no. 09, p. 46, 2002, doi: https://doi.org/10.15407/tpwj.

[30] J. Xu *et al.*, "Effect of annealing and cold rolling on interface microstructure and properties of Ti/Al/Cu clad sheet fabricated by horizontal twin-roll casting," *J. Mater. Res. Technol.*, vol. 16, pp. 530–543, 2022, doi: 10.1016/j.jmrt.2021.12.017.

[31] S. Yan and Y. Shi, "Influence of laser power on microstructure and mechanical property of laser-welded Al/Cu dissimilar lap joints," *J. Manuf. Process.*, vol. 45, no. 7089, pp. 312–321, 2019, doi: 10.1016/j.jmapro.2019.07.009.

[32] J. Chen *et al.*, "Effect of substrates on the formation of Kirkendall voids in Sn/Cu joints," *Weld. World*, vol. 63, no. 3, pp. 751–757, 2019, doi: 10.1007/s40194-019-00704-5.

[33] C. Wang *et al.*, "Quantitative analysis of microstructural evolution at Cu/Al solid-liquid bonding interface," *Xiyou Jinshu Cailiao Yu Gongcheng/Rare Met. Mater. Eng.*, vol. 47, no. 4, pp. 1037–1042, 2018, doi: 10.1016/s1875-5372(18)30116-4.

[34] G. Neumann and C. Tuijn, *Self diffusion and impurity diffusion in pure metals*, vol. 24, no. 03. 2017.

[35] H. Li *et al.*, "Interfacial bonding mechanism and annealing effect on Cu-Al joint produced by solid-liquid compound casting," *J. Mater. Process. Technol.*, vol. 252, pp. 795–803, 2018, doi: 10.1016/j.jmatprotec.2017.10.050.

[36] R. Zhang *et al.*, "Effect of heat treatment on the interface of Al/Cu bimetal laminated material," *Ordnance Mater. Sci. Eng*, vol. 34, no. 5, pp. 5–8, 2011.

[37] X. Zhou *et al.*, "Microstructures and mechanical behavior of aluminum-copper lap joints," *Mater. Sci. Eng. A*, vol. 705, pp. 105–113, 2017, doi: 10.1016/j.msea.2017.08.056.
[38] Q. Shen *et al.*, "Microstructure and mechanical properties of TC4/oxygen-free copper joint with silver interlayer prepared by diffusion bonding," *Mater. Sci. Eng. A*, vol. 596, pp. 45–51, 2014, doi: 10.1016/j.msea.2013.12.017.
[39] F. an Hua, H. wu Song, T. Sun, and J. ping Li, "Inter-diffusion based analytical model for growth kinetics of IMC layers at roll bonded cu/al interface during annealing process," *Met. Mater. Int.*, vol. 26, no. 3, pp. 333–345, 2020, doi: 10.1007/s12540-019-00333-z.
[40] Y. Xiao *et al.*, "Combinatorial investigation of Al–Cu intermetallics using small-scale mechanical testing," *J. Alloys Compd.*, vol. 822, p. 153536, 2020, doi: 10.1016/j.jallcom.2019.153536.
[41] I. Galvão, A. Loureiro, and D. M. Rodrigues, "Critical review on friction stir welding of aluminium to copper," *Sci. Technol. Weld. Join.*, vol. 21, no. 7, pp. 523–546, 2016, doi: 10.1080/13621718.2015.1118813.
[42] X. G. Wang, X. G. Li, F. J. Yan, and C. G. Wang, "Effect of heat treatment on the interfacial microstructure and properties of Cu-Al joints," *Weld. World*, vol. 61, no. 1, pp. 187–196, 2017, doi: 10.1007/s40194-016-0393-x.
[43] F. J. Gil, M. P. Ginebra, J. M. Manero, and J. A. Planell, "Formation of α-Widmanstätten structure: effects of grain size and cooling rate on the Widmanstätten morphologies and on the mechanical properties in Ti6Al4V alloy," *J. Alloys Compd.*, vol. 329, no. 1, pp. 142–152, 2001, doi: https://doi.org/10.1016/S0925-8388(01)01571-7.